

## Study on Constitutive Model for Root System of Korshinsk peashrub in Axial Tension

Guojian Feng\*, Jun Du, Weiwei Zhu, Zhigang Qiu

School of Urban and Rural Construction & Engineering Management  
Kunming University  
Kunming 650214, China  
E-mails: [fengguojian2000@163.com](mailto:fengguojian2000@163.com), [dujun0605@126.com](mailto:dujun0605@126.com),  
[zwwwswfc@126.com](mailto:zwwwswfc@126.com), [qiuzhigang317@qq.com](mailto:qiuzhigang317@qq.com)

\*Corresponding author

Received: June 23, 2015

Accepted: November 16, 2015

Published: December 22, 2015

**Abstract:** Constitutive model for root system of Korshinsk peashrub (*Caragana korshinskii* Kom.) in axial tension is an important tool for analyzing the mechanism of soil reinforcement of root system. This model enables a mechanical analysis on strength and deformation of root system and root-soil complex. We carried out axial tension test of root system of Korshinsk peashrub in this paper and discussed the stress-strain relation. Based on the experimental results, the constitutive model for root system of Korshinsk peashrub in axial tension was established. Results showed that: (1) When the strain was smaller than 4%, the stress-strain relation was linear for single root, corresponding to linear elastic deformation; when the strain was larger than 4%, the single root underwent plastic deformation; (2) Elastic modulus of the root system was related to root diameter by a power function. The smaller the root diameter, the higher the elastic modulus was; (3) Root diameter was related to the ultimate tensile strength of root also by a power function. The smaller the root diameter, the higher the ultimate tensile strength of root was; (4) The tensile stress-strain curve of the root system divided into ascending segment and descending segment, which was fitted by parabola and curvilinear model, respectively.

**Keywords:** Root system, Tensile test, Stress-strain curve, Constitutive model.

### Introduction

Landslide, debris flow and other geological disasters can threaten people's life and cause huge economic loss and ecological damage. The prevention and management of these geological disasters are usually based on grouted rubble, dry masonry and sprayed concrete. These methods are costly and have poor aesthetic effect. Recently, the soil reinforcement capacity of root system has drawn much attention as the root system is believed to enhance slope stability. Forming root-soil complex, the root system of plants will undergo tensile deformation under shear stress when there is deformation of slope or even landslide. Thus the root system of plants is subjected to tension, and the probability of root system being in tension is larger than being under shear stress. Some researchers have carried out tests on the tensile properties of root system of plants. Abernethy and Rutherford [1] believed that the root system of plants had high tensile strength which increased soil stability. Cofie and Koolen [7] found that the tensile rate had an influence on tensile strength of the root system. As the tensile rate increased from 10/min to 400/min, the tensile stress increased by 8%-20%. Genet et al. [9] conducted tensile test on fresh roots of five plants, which were ranked in a decreasing order of tensile strength: *Fagus sylvatica*, *Picea abies*, *Castanea sativa*, *Pinus pinaster* and *Pinus nigra austriaca*. On the microscopic scale, it was found that the content of cellulose in root system affected tensile strength and the two were positively correlated.

Bischetti et al. [3] and Mattia et al. [17] studied the tensile performance of root system of trees and shrubs, concluding that the tensile strength of single root was in reverse proportion to root diameter. Tosi [19] measured the tensile strength of root system of 3 shrub species in the north of Ya Ning Peninsula, Italy. It was found that the tensile strength of root system was related to diameter by a quadratic polynomial equation. The tensile strength of the root system decreased with increasing root diameter, and this relation could be described by a power function. De Baets et al. [8] performed tensile tests on root system of 25 Mediterranean plant species, and the tensile strength varied for each plant species. In herbal plants, the root system of *Brachypodium* species had the highest tensile strength, and *Festuca* species had the smallest tensile strength. In shrubs, the root system of *Salsola collina* had the highest tensile strength, while the root system of *Nerium oleander* had the smallest tensile strength. In trees, the root system of *Tamarix ramosissima* had a higher tensile strength. Li [12] studied four slope protection herbal plants in loess area of Qinghai-Tibet Plateau. Having an average diameter of about 0.25 mm, the root system of *Elymus dahuricus*, *Agropyron trachycaulum*, *Leymus secalinus*, *Achnatherum splendens* had higher tensile strength. The tensile strength of root system of *Achnatherum splendens* reached as high as 82.55 MPa, and it increased with the root diameter, though the variation was described by different function. Yuan [21] and Yuan et al. [22] found that in two growth periods, the tensile strength of root system of *Artemisia sphaerocephala krasch* was negatively correlated with root diameter by a power-exponential function. Wang [20] performed tensile tests on the root system of *Festuca elata*, *Lolium*, *Cynodon dactylon* and *Poa pratensis* L. It was pointed out that stress-strain relation of the root system of the first two plant species corresponded to non-linear elastic deformation and the roots were elastoplastic. For the last two plant species, the stress-strain relation of the root system obeyed Hooke's law and was linear, so the roots were plastic. Li et al. [14] investigated the tensile mechanical properties of root system of *Larix principis-rupprechtii* Mayr. under different root length and diameter and with or without peeling. The stress-strain relation of the root system of this plant presented as a unimodal curve without obvious neck, and thus the roots were elastoplastic. Chen et al. [5] carried out pullout test on the root system of 7 plant species to understand the stress-strain relation, namely, *Abies fabric*, *Rhododendron*, *Populus purdomii*, *Betula utilis*, *Sorbus pohuashanensis*, *Viburnum dilatatum Thunb* and *Euonymus alatus*. It was concluded that pullout test can be used to determine stress-strain relation. The stress-strain relation of the root system of the above plant species was fitted by hyperbolic curve and parabola, respectively. The stress-strain curve fitting using hyperbola had a larger error, while that using parabola was better. Ali et al. [2] designed a system to provide a flexible and usable web environment for defining and running bioinformatics analyses for the ease of researchers working in plants sciences. This system embeds simple yet powerful data management features that allow the user to reproduce analyses and to combine tools using an adobe flex tool. Kosturkova and Delinick [11] indicated that potentized nanodilutions (PNDs) of metallic copper have biological effects on pea seed development which are similar to the effect of copper (water solutions of  $\text{CuSO}_4$ ) and the PNDs can stimulate response for overcoming the stress applied to seeds. We performed uniaxial tension test on root system of Korshinsk peashrub in this paper and fitted the stress-strain curve based on experiment data. The constitutive model for root system of Korshinsk peashrub in tension was built and used for describing the tensile deformation of root system. The findings of this study can provide reference for slope protection design and construction.

## Equipments and materials

### *Equipments*

YG(B)026H Electronic Fabric Strength Tester (resolution 0.1 N, measuring scope 0-2500 N) was used. This equipment was composed of rack, transmission lifting mechanism, strain gauge, upper and lower clamp, electronic control cabinet and display panel. The upper clamp was connected to the strain gauge, and the lower clamp to the pedestal.

### *Materials*

Korshinsk peashrub (*Caragana korshinskii* Kom.) has good resistance to drought, cold and high temperature and can grow on extremely infertile soil. Korshinsk peashrub has become one of the major tree species for water and soil conservation and stabilization for sands by afforestation in China due to its adaptability to extreme environment. The experimental material was the wild Korshinsk peashrub growing on the slope of the campus of Kunming University (average altitude 1894 m, 25°02' N, 102°42' E). The annual average temperature of the experiment site is about 15 °C with annual average precipitation of 1000 mm. The Korshinsk peashrub collected was initially grown on red clay soil. The slope gradient is 50°-55°, and the vegetation cover is 70% with shrubs and grasses as the predominant communities. The hydrogeological background is simple, and the recharge mainly comes from atmospheric precipitation and surface runoff. The 0.5a fresh root system of Korshinsk peashrub was acquired by excavating the whole plant. With the plant situated at the center of circle, a ditch about 2 m in depth was dug with the radius of 2 m. The soil on which the plant was grown was removed gradually until the entire plant was excavated. To ensure the freshness, the root system was preserved in humid soil to simulate the original growth environment. The root system was taken back to laboratory immediately for tensile test.

### *Experimental method*

The root system was placed between the upper and lower clamps of the tester. According to the protocol, the root length was taken as 5-10D (*D* is root diameter). In this experiment, the root length was 60 mm. After start-up, the tensile rate was set as 500 mm/min until the root system was fractured. During test, the part of root system in the clamping head was the zone of stress concentration and was vulnerable to fracture. Besides, the root system might be dislocated from the clamp. The data of these two parts of root system were removed. The root diameter at the site of fracture was measured with vernier caliper, and the tensile force of fracture was recorded. Thus the tensile stress is calculated by

$$\sigma = \frac{4F}{\pi D^2} \quad (1)$$

where  $\sigma$  is the tensile stress of root system (MPa);  $F$  is the maximum tensile strength (N);  $D$  is root diameter at the site of fracture (mm).

The strain  $\varepsilon$  of root system is calculated by

$$\varepsilon = \frac{\Delta l}{l} \quad (2)$$

where  $\varepsilon$  is the strain of root system, which is a dimensionless quantity;  $\Delta l$  is deformation (mm) in tension test;  $l$  is the initial length of root before test (mm), taken as 60 mm.

### Statistical analysis

The root diameter-stress relation was fitted by using CurveExpert1.4 based on the experiment data; the stress-strain curves and diameter-stress curves of the root system were fitted by OriginLab.

## Results

### Stress-strain curve

The stress-strain curves under each diameter were plotted using OriginLab, as shown in Fig. 1. It can be seen that at the early stage of tensile test, i.e., the strain was less than 4%, the stress-strain relation was linear for single root. At this stage, linear elastic deformation dominated, and Hooke's law was obeyed. The slope of the line represented elastic modulus  $E$  of the root system. After that, when the strain was above 4%, the stress-strain relation was approximately linear for single root as the stress increased. However, the slope of this linear segment was smaller than that in linear elastic stage. This indicated that plastic deformation dominated after the elastoplastic stage.

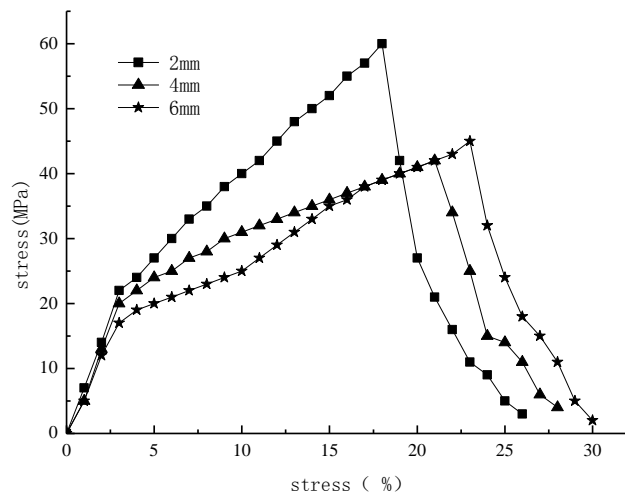


Fig. 1 Stress-strain curve of root system

The stress-strain curves varied for each diameter class due to different content of each root component and ultimate tensile strength. The root components that are damaged sequentially from outer to inner layer are periderm, secondary phloem and secondary xylem. The tough and elastic phloem fibers in secondary phloem will be constantly stretched under increasing tensile force, showing elastic deformation. This corresponded to linear segment in Fig. 1 with strain less than 4%. As the tensile force continued to increase, the wood fibers in xylem were subjected to tension. Since the wood fibers were brittle, the root system would present non-linear elastic deformation, corresponding to the linear segment in Fig. 1 with strain above 4%. Thus the roots of Korshinsk peashrub were elastic at the early stage of tensile test, showing linearity in stress-strain relation. When the tensile force exceeded the elastic limit, the root system showed plastic deformation. The stress increased rapidly with increasing strain.

### Elastic modulus

It can be seen from Fig. 1 that when the strain of the root system was less than 4%, the stress-strain relation was linear. Thus the root system showed elastic deformation, which obeyed Hooke's law. The slope of the line within elastic limit represented elastic modulus  $E$  of the root system. Using experiment data and Fig. 1, the elastic modulus for each diameter

was calculated, as shown in Table 1.

Table 1. Elastic modulus of root system for each diameter

Root diameter, (mm)	2	4	6
Elastic modulus, (MPa)	733	667	566

Since the tensile force applied in test was along the fibers of the root system, elastic modulus was a measure of the tensile strength of root system along the fibers to some extent. The larger the elastic modulus, the higher the rigidity and the smaller the deformation was. As shown in Table 1, the smaller the root diameter, the larger the elastic modulus, which indicated good linear elastic performance of single root with smaller diameter. Elastic modulus  $E$  was related to diameter  $D$  by a power function, fitted as  $E = 861.62D^{-0.22}$ ,  $R^2 = 0.95$ . This was consistent with the elastic modulus-root diameter relation fitted by Chen et al. [4] for *Pinus tabuliformis*, *Betula platyphylla*, *Larix gmelinii* and *Quercus mongolica*. The reasons may lie in the percentage content of phloem fibers and wood fibers, degree of lignification periderm and rate of lignification [25].

#### Relation between root diameter and stress

As shown in Fig. 1m the smaller the root diameter, the larger the maximum stress it withstood before failing was. When the root diameter was 2 mm, the maximum stress was 60 MPa; when root diameter was 6 mm, the stress was 45 MPa. This result indicated that the fibrous roots should have higher tensile strength. The relation of root diameter with maximum stress varied for each plant species. For *Salix mongolica*, *Sabina vulgaris*, *Larix gmelinii* and *Quercus mongolica*, the maximum stress before failing (ultimate tensile strength) is related to root diameter by a power function; for *Sarcozygium xanthoxylon Bunge* and *Nitraria tangutorum*, the relation was exponential [10, 13, 18, 24]. For *Cynodon dactylon*, *Trifolium repens* and *Amorpha fruticosa*, the relation between tensile strength and root diameter can be fitted by linear, polynomial, logarithmic and exponential mode, respectively [6]. The curves showing the relation between root diameter and maximum stress for Korshinsk peashrub were plotted in Fig. 2 using CurveExpert1.4. The curves represented power function  $\sigma = 86.9 \times D^{-5.13}$ ,  $R^2 = 0.87$ . This agreed with the conclusions by Luo et al. [15] and Lv et al. [16]. Many researchers have demonstrated that ultimate tensile strength of single root of plant decreases with the increasing root diameter, though the mechanism is unclear. Some researchers believe that the content of cellulose per unit dry mass is higher in roots with smaller diameter [9, 23]. However, they did not separate cellulose from holocellulose, and the content of the latter varies in root system of different plant species. Therefore, the influence of cellulose content on tensile strength of root system needs to be further investigated.

#### Constitutive model for root system in tension

It can be seen from Fig. 1 that the curve has two segments, the segment corresponding to elastoplastic deformation and the descending segment. The data in Fig. 1 were treated by nondimensionalization. The  $\varepsilon_a/\varepsilon_0$  and  $\sigma/\sigma_0$  were plotted on  $x$  axis and  $y$  axis of the new coordinate system, respectively. The elastoplastic deformation was fitted by parabolic model, and the descending segment by curvilinear model. Thus the constitutive model is obtained:

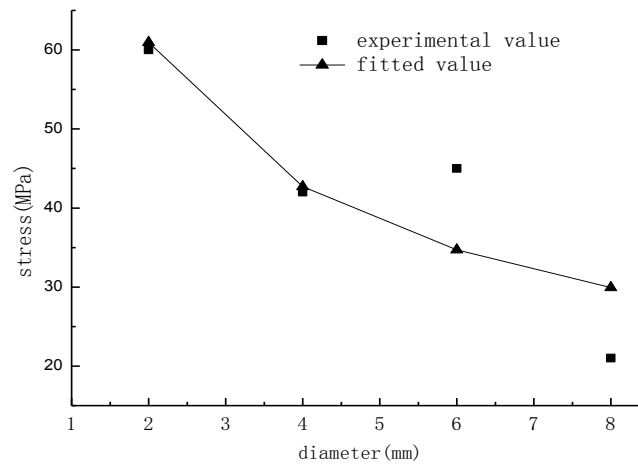


Fig. 2 Root diameter-stress curve

$$\frac{\sigma}{\sigma_0} = \begin{cases} A_1 \times \frac{\varepsilon_a}{\varepsilon_0} - B_1 \times \left( \frac{\varepsilon_a}{\varepsilon_0} \right)^2 & \text{elastoplastic stage} \\ \frac{A_2 \times \frac{\varepsilon_a}{\varepsilon_0} + B_2}{C_1 \times \left( \frac{\varepsilon_a}{\varepsilon_0} \right)^2 + D_1 \times \frac{\varepsilon_a}{\varepsilon_0} + 1} & \text{descending segment} \end{cases} \quad (3)$$

where  $\sigma$  is tensile stress of root system;  $\sigma_0$  is maximum tensile stress;  $\varepsilon_a$  is strain of root system;  $\varepsilon_0$  is the strain corresponding to maximum tensile stress;  $A_1$ ,  $A_2$ ,  $B_1$ ,  $B_2$ ,  $C_1$  and  $D_1$  are experimental parameters.

The data of elastoplastic stage were treated using Eq. (3), and the fitting was done using CurveExpert1.4. For the descending segment, 4 boundary conditions were needed to determine 4 unknown quantities: 1) the curve passes through the peak point, i.e. when  $\varepsilon_a / \varepsilon_0 = 1$ ,  $\sigma / \sigma_0 = 1$ , by substituting into the equation of descending segment, there is  $A_2 + B_2 = C_1 + D_1 + 1$ ; 2) the curve has extreme values at the peak point, i.e., by finding the derivative of the curve, the value is 0 at point (1, 1). After substituting into the equation of descending segment, there is  $A_2 C_1 + 2B_2 C_1 - A_2 + B_2 D_1 = 0$ . Since the equation of descending segment contains 4 unknowns, 2 boundary conditions are not sufficient to obtain all parameters. Therefore, the coordinates of the point of inflection and point of convergence are needed on the descending segment.

The curve passes through the point of inflection, thus

$$\left( \frac{\sigma}{\sigma_0} \right)_{pi} = \frac{A_2 \times \left( \frac{\varepsilon_a}{\varepsilon_0} \right)_{pi} + B_2}{C_1 \times \left( \frac{\varepsilon_a}{\varepsilon_0} \right)_{pi}^2 + D_1 \times \left( \frac{\varepsilon_a}{\varepsilon_0} \right)_{pi} + 1}$$

The curve passes through the point of convergence, thus

$$\left(\frac{\sigma}{\sigma_0}\right)_{pc} = \frac{A_2 \times \left(\frac{\varepsilon_a}{\varepsilon_0}\right)_{pc} + B_2}{C_1 \times \left(\frac{\varepsilon_a}{\varepsilon_0}\right)_{pc}^2 + D_1 \times \left(\frac{\varepsilon_a}{\varepsilon_0}\right)_{pc} + 1}$$

Substituting 4 boundary conditions into the equation of the descending segment, 4 unknowns are obtained:

$$A_2 = 2C_1 + D_1; \quad B_2 = 1 - C_1; \quad C_1 = \frac{c_1 b_2 - c_2 b_1}{a_1 b_2 - a_2 b_1}; \quad D_1 = \frac{a_1 c_2 - a_2 c_1}{a_1 b_2 - a_2 b_1},$$

where

$$a_1 = x_{pi}^2 y_{pi} - 2x_{pi} + 1; \quad b_1 = x_{pi}(y_{pi} - 1); \quad c_1 = 1 - y_{pi};$$

$$a_2 = x_{pc}^2 y_{pc} - 2x_{pc} + 1; \quad b_2 = x_{pc}(y_{pc} - 1); \quad c_2 = 1 - y_{pc}.$$

The coordinates of the point of infection and point of convergence on the descending curve are shown in Table 2. Thus the parabolic model and the curvilinear model for each diameter class are derived and shown in Table 3.

Table 2. Coordinates of point of infection and point of convergence in descending segment

Diameter class	$x_{pi}$	$y_{pi}$	$x_{pc}$	$y_{pc}$
<b>2 mm</b>	1.11	0.45	1.44	0.05
<b>4 mm</b>	1.14	0.36	1.33	0.1
<b>6 mm</b>	1.22	0.24	1.3	0.04

Note: the angle  $pi$  and  $pc$  below standard symbols represent the point of infection and point of convergence respectively

Table 3. Parameters of constitutive model for tension under different diameter class

		Diameter		
		2 mm	4 mm	6 mm
Elastoplastic stage	$A_1$	1.67	2.27	1.77
	$B_1$	0.73	1.37	0.83
Descending segment	$A_2$	0.00	0.01	-0.12
	$B_2$	0.01	0.00	0.16
	$C_1$	0.99	1.00	0.84
	$D_1$	-1.98	-1.99	-1.80

For diameter class 2 mm, 4 mm and 6 mm, the constitutive models for root system of Korshinsk peashrub in tension are shown in Eqs. (4)-(6), respectively:

$$\frac{\sigma}{\sigma_0} = \begin{cases} 1.67 \times \frac{\varepsilon_a}{\varepsilon_0} - 0.73 \times \left( \frac{\varepsilon_a}{\varepsilon_0} \right)^2 & \text{elastoplastic stage} \\ \frac{0.01}{0.99 \times \left( \frac{\varepsilon_a}{\varepsilon_0} \right)^2 - 1.98 \times \frac{\varepsilon_a}{\varepsilon_0} + 1} & \text{descending segment} \end{cases} \quad (4)$$

$$\frac{\sigma}{\sigma_0} = \begin{cases} 2.27 \times \frac{\varepsilon_a}{\varepsilon_0} - 1.37 \times \left( \frac{\varepsilon_a}{\varepsilon_0} \right)^2 & \text{elastoplastic stage} \\ \frac{0.01 \times \frac{\varepsilon_a}{\varepsilon_0}}{1.00 \times \left( \frac{\varepsilon_a}{\varepsilon_0} \right)^2 - 1.99 \times \frac{\varepsilon_a}{\varepsilon_0} + 1} & \text{descending segment} \end{cases} \quad (5)$$

$$\frac{\sigma}{\sigma_0} = \begin{cases} 1.77 \times \frac{\varepsilon_a}{\varepsilon_0} - 0.83 \times \left( \frac{\varepsilon_a}{\varepsilon_0} \right)^2 & \text{elastoplastic stage} \\ \frac{-0.12 \times \frac{\varepsilon_a}{\varepsilon_0} + 0.16}{0.84 \times \left( \frac{\varepsilon_a}{\varepsilon_0} \right)^2 - 1.80 \times \frac{\varepsilon_a}{\varepsilon_0} + 1} & \text{descending segment} \end{cases} \quad (6)$$

The experimental data and the fitted data are provided in Fig. 3.

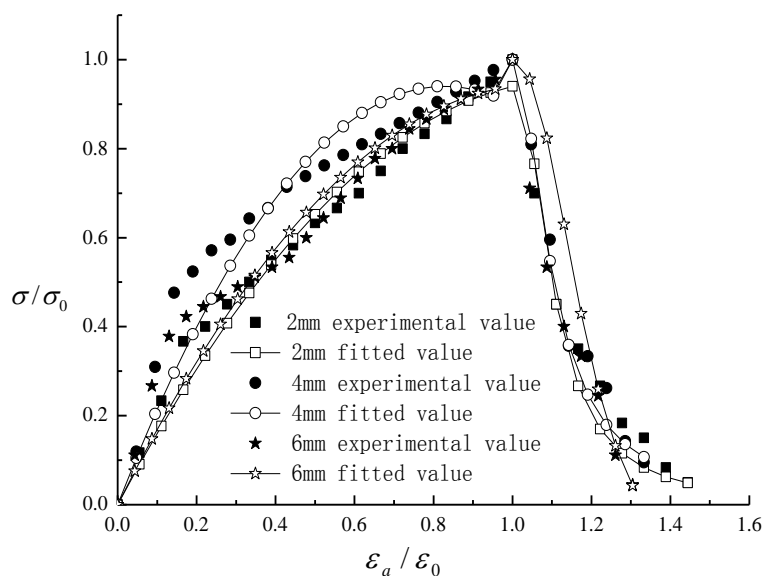


Fig. 3 Constitutive model for root system of Korshinsk peashrub in tension

## Conclusion

Tensile mechanical performance of root system of Korshinsk peashrub is an important factor that maintains slope stability. We performed tensile tests on root system of Korshinsk peashrub with the same length but different diameter (2 mm, 4 mm and 6 mm) using YG(B)026H Electronic Fabric Strength Tester at the same tensile rate. The stress-strain curves for the root system were plotted with the estimation of maximum tensile stress and elastic modulus. The following conclusions were drawn:

- (1) The stress-strain curve consisted of segment corresponding to elastoplastic stage and descending segment. Because of elastic phloem fibers in root system, the root system showed elastic deformation at the beginning. As the tensile force increased, the wood fibers were subjected to tension, and the root system showed plastic deformation because of the brittleness of wood fibers. The slope in the plastic stage was larger than in the elastic stage.
- (2) The smaller the root diameter, the larger the elastic modulus was. The two were negatively correlated by a power function. This may be explained by percentage content of phloem fibers and wood fibers in root, the degree of lignification of periderm and rate of lignification.
- (3) The root diameter was negatively related to maximum tensile stress by a power function. The smaller the diameter (i.e., the higher the content of cellulose per unit dry mass), the higher the maximum tensile stress was.
- (4) The stress-strain curve of root system of Korshinsk peashrub in axial tension consisted of ascending segment and descending segment, which were fitted separately. After nondimensionalization, the ascending segment was fitted by parabolic model, while the descending segment was fitted by curvilinear model using the coordinates of point of reflection and point of convergence.

## Acknowledgement

*Supported by the Key Disciplines (Ecology) Project of Yunnan Education Department, the Scientific Research Funds of Kunming University (XJL14012).*

## References

1. Abernethy B., I. D. Rutherford (2001). The Distribution and Strength of Riparian Tree Roots in Relation to Riverbank Reinforcement, *Hydrological Processes*, 15(1), 63-79.
2. Ali M., R. R. Khalid, M. Nawaz, N. Qamar (2011). Development of a Tool for the Analysis of Plant Stress Proteins, *International Journal Bioautomation*, 15(4), 261-266.
3. Bischetti G. B., E. A. Chiaradia, T. Simonato, B. Speziali, B. Vitali, P. Vullo, A. Zocco (2005). Root Strength and Root Area Ratio of Forest Species in Lombardy (Northern Italy), *Plant and Soil*, 278, 11-22.
4. Chen L., J. Ji, X. Ji, K. Jiang, X. Liu, C. Lv, H. Song, P. Wang, C. Zhao, H. Zhao, S. Zhou (2012). *Basic Mechanical Properties of Forest Root System*, Beijing, Science Press.
5. Chen L., X. Yu, X. Liu, W. Song (2007). Study on the Constitutive Relation of Forest Root System, *Journal of Mountain Science*, 25(2), 224-228.
6. Chen X. (2005). Study on Expressway Slope Eco-protection Technology and Its Application, Master Thesis, Wuhan, Wuhan University of Technology, (in Chinese).
7. Cofie P., A. J. Koolen (2001). Test Speed and Other Factors Affecting the Measurements of Tree Root Properties Used in Soil Reinforcement Models, *Soil and Tillage Research*, 63(1-2), 51-56.

8. De Baets S., J. Poesen, B. Reubens, K. Wemans, J. De Baerdemaeker, B. Muys (2008). Root Tensile Strength and Root Distribution of Typical Mediterranean Plant Species and Their Contribution to Soil Shear Strength, *Plant and Soil*, 305, 207-226.
9. Genet M., A. Stokes, F. Salin, S. B. Mickovski, T. Fourcaud, J.-F. Dumail, R. van Beek (2005). The Influence of Cellulose Content on Tensile Strength in Tree Roots, *Plant and Soil*, 278, 1-9.
10. Geng W., L.-H. Wang, J. Liu, K.-Y. Wang (2008). Study on Three 4-5 Years Shrubs Root Pull-resistance Mechanics in Ordos Plateau, *Journal of Inner Mongolia Agricultural University (Natural Science Edition)*, 29(3), 86-89.
11. Kosturkova G. P., A. N. Delinick (Delinikou) (2007). Development of Plant Model to Study Biological Effects of Nanodilutions, *International Journal Bioautomation*, 8(Suppl. 1), 184-192.
12. Li C. (2008). Study on the Tensile Properties of Single Root of Four Herbaceous Plants in Loess Area of Qinghai-Tibet Plateau, *Science of Soil and Water Conservation*, 5, 33-34.
13. Li S., H. Sun, Z. Yang, L. He, B. Cui (2006). Mechanical Characteristics of Interaction between Root System of Plants and Rock for Rock Slope Protection, *Chinese Journal of Rock Mechanics and Engineering*, 25(10), 2051-2057.
14. Li X., L. Chen, P. Wang (2012). Tensile Mechanical Properties of Roots of *Larix principis-rupprechtii*, *Science of Soil and Water Conservation*, 10(1), 82-87, (in Chinese).
15. Luo L.-Z., S.-C. Li, H.-L. Sun, F. Long, C. Zhang, D.-Q. Lu (2011). Characteristics of Tensile of Root System of *Broussonetia papyrifera* Growing on Lithosol Steep Slopes, *Science of Soil and Water Conservation*, 4, 37-41.
16. Lv C., L. Chen, S. Zhou, P. Wang, X. Ji, X. Zhang (2011). Root Mechanical Characteristics of Different Tree Species, *Transactions of the Chinese Society of Agricultural Engineering*, 27(1), 329-335.
17. Mattia C., G. B. Bischetti, F. Gentile (2005). Biotechnical Characteristics of Root Systems of Typical Mediterranean Species, *Plant and Soil*, 278(1), 23-32.
18. Shi M., D. Wang, R. Li (1994). The Research on Root System Distribution and Tensile Strength of Soil Conservation Bushes in Limestone Area, *Shanxi Forestry Science and Technology*, 1, 17-19.
19. Tosi M. (2007). Root Tensile Strength Relationships and Their Slope Stability Implications of Three Shrub Species in the Northern Apennines (Italy), *Geomorphology*, 87(4), 268-283.
20. Wang H. (2010). Research on Mechanism of Root Reinforcing Soil and Slope Erosion in Slope Protection by Vegetation, Ph.D. Thesis, Chengdu, Southwest Jiaotong University, (in Chinese).
21. Yuan S. (2010). Tensile Strength Characteristics of Single Root of Four Plant Species, Hohhot, Inner Mongolia Agricultural University.
22. Yuan S.-J., G.-Q. Niu, J. Liu, X. Zhang, H.-W. Xing, X.-J. Yao (2008). Instantaneous Anti-tension and Tensile Strength of Single Root of Four Plant Species in Two Growth Periods, *Inner Mongolia Water Resources*, 6, 77-79.
23. Zhao L., B. Zhang (2007). Experimental Study on Root Bio-mechanics and Relevant Factors of *Medicago sativa* and *Digitaria sanguinalis*, *Transactions of the Chinese Society of Agricultural Engineering*, 23(9), 7-12.
24. Zhu H., X. Hu, X. Mao, G. Li, H. Sheng, G. Chen (2008). Studies on Mechanical Characteristics of Shrub Roots for Slope Protection in Loess Area of Tibetan Plateau, *Chinese Journal of Rock Mechanics and Engineering*, 27(Suppl. 2), 3445-3452.

25. Zhu H., X. Hu, X. Mao, G. Li, X. Zhang, G. Chen (2009). Relationship between Mechanical Characteristics and Anatomical Structures of Slope Protection Plant Root, Transactions of the Chinese Society of Agricultural Engineering, 25(5), 40-46, (in Chinese).

**Guojian Feng, M.Sc.**

E-mail: [fengguojian2000@163.com](mailto:fengguojian2000@163.com)



Guojian Feng graduated from Chongqing University, majored in geotechnical engineering. His areas of research are environmental geotechnical and slope. He has awarded with several grants for his research projects. Currently, he is working on several research projects.

**Jun Du, M.Sc.**

E-mail: [dujun0605@126.com](mailto:dujun0605@126.com)



Jun Du graduated from Kunming University of Science and Technology. His areas of research are geological disasters and slope. He is working on several related research projects. He has strong ability of engineering practice.

**Weiwei Zhu, M.Sc.**

E-mail: [zwswfc@126.com](mailto:zwswfc@126.com)



Weiwei Zhu graduated from Nanjing Forestry University. He is working in Kunming University. He has excellent command over different numerical simulation tools and working on several research projects.

**Zhigang Qiu, M.Sc.**

E-mail: [qiuzhigang317@qq.com](mailto:qiuzhigang317@qq.com)



Zhigang Qiu graduated from Tongji University, majored in disaster prevention and mitigation. He has ability on the data analysis and processing. His scientific interests are numerical simulation and seismic analysis.